International Journal of Mechanical Sciences 74 (2013) 91–98

Contents lists available at SciVerse ScienceDirect

International Journal of Mechanical Sciences

journal homepage: www.elsevier.com/locate/ijmecsci

A contact model for orthotropic-viscoelastic materials

N.V. Rodriguez [a,b], M.A. Masen [a,*], D.J. Schipper [a]

[a] Laboratory for Surface Technology and Tribology, Faculty of Engineering Technology, University of Twente, P.O. Box 217, 7500AE Enschede, The Netherlands
[b] Dutch Polymer Institute DPI, P.O. Box 902, 5600AX Eindhoven, The Netherlands

ARTICLE INFO

Article history:
Received 21 September 2012
Received in revised form
2 April 2013
Accepted 11 May 2013
Available online 22 May 2013

Keywords:
Contact mechanics
Orthotropic material
Anisotropy
Viscoelastic material
Fibre-reinforced elastomer

ABSTRACT

In many industrial applications, fibre-reinforced polymers are in contact with rigid surfaces. The contact behaviour of such polymers is both anisotropic and viscoelastic: the polymers exhibit viscoelastic behaviour and the addition of short fibres results in a directionality in the material behaviour of the composite. This work focuses on the contact problem of an orthotropic viscoelastic material in contact with a spherical rigid indenter, in which the radius of the contact area is much larger than the fibre size.

A general form of anisotropic behaviour has been considered in order to describe materials with a high degree of anisotropy. By using separation of variables a solution for the quasi-static contact problem for viscoelastic and generally anisotropic materials is obtained by combining the linear theory of viscoelasticity with the Hertz solution for elastic anisotropic materials as derived by Willis. The developed contact model requires nine elastic material parameters in combination with one time dependent material parameter as input, in order to characterise the behaviour of the material. It is shown that the results of the developed model show good agreement with both isotropic and anisotropic materials described in literature. Furthermore, it is shown that ignoring the anisotropy of a viscoelastic material will result in an overestimate of the stiffness of the material.

1. Introduction

Polymers reinforced with fibres are widely used in industry, where often the polymer-fibre composite is in contact with a rigid counter surface and in relative motion. Because the polymers have properties that are not always desirable, such as low temperature resistance and low stiffness, they are reinforced with fibres. In the same way as the addition of fibres influences the material behaviour, they also modify the contact behaviour and consequently the tribological behaviour of tribo-systems containing these composites. In this work, the contact of a fibre reinforced polymer with a rigid surface is studied. The fibre reinforced polymer is modelled considering viscoelastic material behaviour (due to the polymer matrix) and anisotropic material behaviour (due to the orientation of the fibre in the composite). The rigid surface is considered to be a spherical rigid indenter.

The behaviour of a viscoelastic material in contact with a rigid spherical indenter is commonly modelled as an extension of the Hertz solution [1,2] where the elastic parameters are replaced by the viscoelastic parameters within the linear theory of viscoelasticity. Contact models which include viscoelastic material behaviour were developed, under certain restrictions, by for instance Johnson [1], Lee and Radok [3] and Graham [4,5]. A more general viscoelastic contact model which includes all previous solutions was developed by Ting [6].

The anisotropic behaviour of a material in contact with a rigid spherical indenter is also often modelled after Hertz. Green and Zerna [7], and Dahan and Zarka [8] modelled the contact behaviour between transversally isotropic materials and spherical rigid indenters. Contact models considering higher degrees of anisotropy are less common. Among these, orthotropic materials are described by nine independent elastic parameters and are one of the more common type of anisotropic materials, examples are long fibre reinforced composites. Contact models of orthotropic materials involve numerical solutions due the large amount of parameters. Willis [9] studied the Hertzian problem for anisotropic materials by numerically solving an analytical solution, and Swanson [10] used this procedure to study the orthotropic case. An approximation of the contact model for orthotropic materials was developed by Yang and Sun [11] and Tan and Sun [12]. They assumed that the contact area and indentation depth for an orthotropic material could be derived from the isotropic case, replacing the isotropic modulus by the modulus in the loading direction.

Swanson [10] made a comparison between two different anisotropic contact models: the approximate anisotropic contact model of Yang and Sun [11] and Tan and Sun [12] and the orthotropic contact model by Willis [9]. It was concluded that, for low degrees of

* Corresponding author at: Laboratory for Surface Technology and Tribology, Faculty of Engineering Technology, University of Twente, P.O. Box 217, 7500AE Enschede, The Netherlands. Tel.: +31 53 489 4390.
E-mail address: m.a.masen@utwente.nl (M.A. Masen).

0020-7403/$ - see front matter © 2013 Elsevier Ltd. All rights reserved.
http://dx.doi.org/10.1016/j.ijmecsci.2013.05.001

Nomenclature

Roman symbols

$A(t)$	time dependent contact area (m^2)
a_x, a_y	half widths of the elliptical contact area (m)
$a_x(t)$, $a_y(t)$	time dependent half widths of the contact area (m)
$\overline{a}(t)$	dimensionless time dependent contact area (–)
$a(t)$	time dependent radius of the contact area (m)
E	elastic modulus (Pa)
E_x,E_y,E_z	elastic modulus in x-, y- and z-direction, respectively (Pa)
F_N	applied normal force (N)
$F_N(t)$	time dependent applied normal force (N)
$\overline{F}(t)$	dimensionless time dependent applied normal force (–)
$f(t)$	auxiliary function $f(t)=\overline{p}(t)/\overline{a}(t)$ (–)
$f^{-1}(t)$	inverse of the auxiliary function $f(t)$ (–)
G	shear modulus (Pa)
G_{yz}, G_{zx}, G_{xy}	shear modulus in the planes yz, zx and xy, respectively (Pa)
$H(t)$	heaviside function (–)
I_1, I_2	contour integrals that encapsulate the material properties in an anisotropic material, defining the contact behaviour (Pa^{-1})
$\overline{p}(t)$	dimensionless time dependent pressure distribution (–)
p_0	maximum contact pressure (Pa)
R	radius of the indenter (m)
t	time (s)
t_*	dummy variable of the convolution integral (s)
$\mathbf{u}$	displacement field vector (m)
$u_i(x_i)$	displacement field depending on spatial variables (m)
$\overline{u}(t)$	normalised time function of the displacement field (–)
$\tilde{u}_z$	Fourier transform of the normal component of the displacement field
u_z	normal component of the displacement field (m)
x, y, z	spatial variables, x and y are in the indentation plane and z is along the direction of indentation

Greek symbols

$\delta(t)$	time dependent indentation depth (m)
δ	indentation depth (m)
$\delta(x)$	Dirac delta function
$\varepsilon(t)$	time dependent strain (–)
ε_{ij}, $\boldsymbol{\varepsilon}$	strain tensor (–)
λ_i	retardation time of the creep compliance coefficient i (s)
ν	Poisson's ratio (–)
$\sigma(t)$	time dependent stress (Pa)
σ_{ij}, $\boldsymbol{\sigma}$	stress tensor (Pa)
$\phi(t)$	creep compliance function (Pa^{-1})
$\overline{\phi}(t)$	normalised creep compliance (–)
ϕ_r	creep compliance at fully relaxed state (Pa^{-1})
ϕ_i	creep compliance coefficient i (Pa^{-1})
$\psi(t)$	stress relaxation function (Pa)
$\overline{\psi}(t)$	normalised stress relaxation (–)
$\psi_{ijkl}(t)$	stress relaxation of the material in 3-D (Pa)

anisotropy, the approximate anisotropic contact model offers a good agreement with the results of the orthotropic contact model. Rodriguez et al. [13] extended this approach to viscoelastic materials, developing a contact model for viscoelastic anisotropic materials with low anisotropy ($E_z/E_x<2$). In the present study, a more general viscoelastic anisotropic contact model is presented, valid for higher degrees of anisotropy. The anisotropic behaviour is modelled following the procedure of Willis [9] and Swanson [10]. This solution is combined with the solution of the viscoelastic contact model from Ting [6], under the assumption of separation of spatial and time variables. Therefore this contact model requires nine elastic parameters, which give the information about the anisotropy of the material, and only one time dependent function, which gives information about the viscoelastic behaviour of the material. Under this assumption, the solution of the contact problem describes a smooth and rigid spherical indenter against an orthotropic viscoelastic-isochronous material, meaning that the properties of the material are time dependent and are described by one time function.

1.1. Coordinate system

To facilitate the discussion regarding the anisotropy of the material, a system of coordinates is defined according to Fig. 1. The direction of indentation corresponds to the positive z-axis, whilst the x–y plane is the plane of initial contact.

2. Elastic orthotropic contact

Willis [9] developed a model describing the anisotropic elastic contact for a point load, and extended this to consider a pressure distribution. The details of this procedure can be found in Appendix A. The contact area is given by an ellipse with principal axes a_x and a_y, defined as

$$a_x=\left(\frac{3RF_N}{4}\right)^{1/3} I_1^{1/3} \text{ and } a_y=\left(\frac{3RF_N}{4}\right)^{1/3} \frac{I_2^{1/2}}{I_1^{1/6}} \tag{1}$$

These expressions are similar to the solution by Hertz presented in [1]. The only difference is in the term representing the elastic material properties, with I_1 and I_2 the numerical solutions of two contour integrals. These depend on the nine material properties of the orthotropic material and are defined in Eqs. (2) and (3) , where $\varepsilon=a_x/a_y$ and $\tilde{u}_z$ is the Fourier transform of the normal displacement due to a point load and depends on all the material properties. Details are given in Appendix A.

$$I_1=\int_0^{2\pi} \tilde{u}_z(\varepsilon\cos\theta, \sin\theta)(\cos\theta)^2 d\theta \tag{2}$$

$$I_2=\int_0^{2\pi} \tilde{u}_z(\varepsilon\cos\theta, \sin\theta)(\sin\theta)^2 d\theta \tag{3}$$

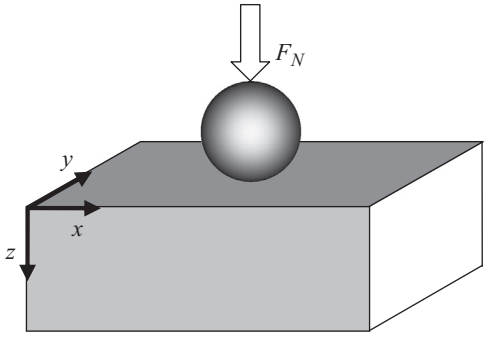

Fig. 1. Schematic of the coordinate system used.

3. Extension to viscoelasticity

To obtain a solution to the viscoelastic orthotropic contact problem, first the auxiliary problem of a concentrated point load applied to a viscoelastic orthotropic half-space is solved, similar to the procedure of Willis [9]. The solution involves the separation of time and space variables; the temporal solution is obtained, and the applied spatial solution corresponds to the solution of Willis [9]. To calculate the contact problem of a viscoelastic anisotropic material indented by a rigid spherical indenter, the contact area and pressure distribution used are the ones defined by Willis [9].

3.1. Solution of a point load in an anisotropic viscoelastic material

Following Willis [9], Swanson [10] and Ting [6], the equations to solve are

- The stress and displacement, which must satisfy equilibrium

$$\frac{\partial \sigma_{ij}(x_i,t)}{\partial x_j}=0 \tag{4}$$

- The strain-displacement relation

$$\varepsilon_{ij}=\frac{1}{2}\left(\frac{\partial u_i}{\partial x_j}+\frac{\partial u_j}{\partial x_i}\right) \tag{5}$$

- The linear viscoelastic stress–strain relation, valid for anisotropic materials:

$$\sigma_{ij}(x_i,t)=\int_0^t \psi_{ijkl}(t-t_*)\frac{\partial \varepsilon_{kl}(x_i,t_*)}{\partial t_*}dt_* \tag{6}$$

Where $\psi_{ijkl}(t)$ is a fourth order time-dependent tensor that corresponds to the stress relaxation functions of the material. The indices indicate the x-, y- and z-directions, and x_i denotes the spatial variable, i.e. $x_x=x$, $x_y=y$ and $x_z=z$.

It is considered that there is full contact between the half-space and the indenter, i.e. no separation occurs within the contact area. Furthermore, inertia is neglected, reducing the problem to a quasi-static one. Assuming the separation of space and time variables enables the definition of the displacement field u, the strain ε and the stress σ, respectively

$$u_i(x_i,t)=u_i(x_i)\overline{u}(t) \tag{7}$$

$$\varepsilon_{ij}(x_i,t)=\varepsilon_{ij}(x_i)\overline{u}(t) \tag{8}$$

$$\sigma_{ij}(x_i,t)=\sigma_{ij}(x_i)\overline{F}(t) \tag{9}$$

where $\overline{u}(t)$ and $\overline{F}(t)$ indicate the time functions of the displacement field and the applied load, respectively. These functions are dimensionless, meaning that the dimension is kept by the spatial variables. The dimensionless applied normal load, $\overline{F}(t)$, is defined by the Heaviside step function as

$$\overline{F}(t)=H(t)=\begin{cases}0 & t<0\\ 1 & t\geq 0\end{cases} \tag{10}$$

For $t<0$, the viscoelastic half-space is stress-free and at $t\geq 0$ the spherical indenter is pressed into the half-space. Similar to Eqs. (7)–(9), it is possible to rewrite $\psi_{ijkl}(t)$as

$$\psi_{ijkl}(t)=\overline{\psi}(t)\cdot\psi_{ijkl} \tag{11}$$

where $\overline{\psi}(t)$ represents a normalised stress relaxation function, describing the time-dependency of the material properties and the constant tensor ψ_{ijkl} behaves similar to the stiffness tensor of the material. This enables the use of ψ_{ijkl} as the common stiffness tensor found in elasticity and therefore the stress–strain relationship in spatial variables can be defined as $\sigma_{ij}(x_i)=\psi_{ijkl}\cdot\varepsilon_{kl}$.

To solve the time dependent component of the displacement field, $\overline{u}(t)$, one of the stress boundary conditions is used, which is defined in both the spatial and temporal variables

$$\sigma_{zz}(x,y,z=0,t)=-\delta(x)\delta(y)F_N\overline{F}(t) \tag{12}$$

where δ refers to the Dirac delta function with reciprocal dimensions to the dimension of x or y. The temporal boundary condition used is then

$$\int_0^t \overline{\psi}(t-t_*)\frac{\partial \overline{u}(t_*)}{\partial t_*}dt_*=\overline{F}(t) \tag{13}$$

Inverting the time dependent boundary condition of Eq. (13), the time dependency of the displacement field $\overline{u}(t)$ can be described by

$$\overline{u}(t)=\int_0^t \overline{\phi}(t-t_*)\frac{\partial}{\partial t_*}H(t_*)dt_*=\overline{\phi}(t) \tag{14}$$

in which the normalised creep compliance function $\overline{\phi}(t)$ is related to the normalised stress relaxation function $\overline{\psi}(t)$ by

$$\int_0^t \overline{\psi}(t-t_*)\overline{\phi}(t_*)dt_*=t \tag{15}$$

The solution of the spatial displacement in the Fourier domain is obtained identically to Willis [9], as described in Eq. (A.9) in Appendix A.

3.2. Solution of the contact problem

The time dependent pressure distribution in the contact is described in terms of the peak contact pressure p_0 by Eq. (16), where the contact area is an ellipse with principal axes $a_x(t)$ and $a_y(t)$. The two principal axes of the contact area show identical time dependency and can be written as $a_x(t)=a_x\,\overline{a}(t)$ and $a_y(t)=a_y\,\overline{a}(t)$. The time dependency of the pressure distribution is given by the dimensionless parameter $\overline{p}(t)$

$$p(x,y,t)=\overline{p}(t)p_0\left(1-\left(\frac{x^2}{a_x\overline{a}(t)}+\frac{y^2}{a_y\overline{a}(t)}\right)\right)^{1/2} \tag{16}$$

The superposition of the spatial and temporal solutions for the normal displacement is given by Eq. (17), where $\overline{u}(t-t_*)$ is the dimensionless time-dependent displacement field at time t, due to a contact pressure that occurred at an instant t_*, and η_1 and η_2 are cos(θ) and sin(θ), respectively.

$$u_z(x,y,0,t)=\int_0^t \frac{\overline{p}(t_*)}{\overline{a}(t_*)}\frac{\partial \overline{u}(t-t_*)}{\partial t_*}dt_*\cdot\frac{\pi p_0 a_y}{4}\int_0^{2\pi}\tilde{u}_z(\varepsilon\eta_1,\eta_2)\times\left[1-\left(\frac{\eta_1 x}{a_x}+\frac{\eta_2 y}{a_y}\right)^2\right]d\theta \tag{17}$$

The first integral on the right side of the equation represents the temporal solution, whilst the second integral is the spatial solution for the orthotropic contact.

The time-dependent, quasi-static relative displacement of the indenter into the half space is given by δ(t) in

$$u_{z-\text{indenter}}+u_{z-\text{half}-\text{space}}=\delta(t)-(Ax^2+By^2+2Cxy)F_N\,\overline{F}(t) \tag{18}$$

For the special case of a rigid spherical indenter, the terms A, B and C in Eq. (18) are [1].

$$A=B=\frac{1}{2R}\quad C=0 \tag{19}$$

Recognising terms between Eqs. (17) and (18) gives

$$\frac{F_N\overline{F}(t)}{2R}=\int_0^t \frac{\overline{p}(t_*)}{\overline{a}(t_*)}\frac{\partial \overline{u}(t-t_*)}{\partial t_*}dt_*\cdot\frac{\pi p_0 a_y}{4a_x^2}\int_0^{2\pi}\tilde{u}_z(\theta)\cos^2(\theta)d\theta \tag{20}$$

Applying an auxiliary function f(t) as defined in Eq. (21)

$$f(t)=\frac{\overline{p}(t)}{\overline{a}(t)} \tag{21}$$

and by using the commutative properties of convolution, it is possible to invert the time dependent terms of Eq. (20), obtaining a solution for the time dependency of the contact area

$$\int_0^t f^{-1}(t-t_*)\frac{\partial H(t_*)}{\partial t_*}dt_* = f^{-1}(t)=\overline{u}(t)=\phi(t) \tag{22}$$

where $f^{-1}(t)$ is the inverse function of f(t). The time-dependent part of the peak contact pressure can be replaced by the time-dependent part of the total contact force, as

$$\overline{F}(t)=\overline{p}(t)\overline{a}^2(t) \tag{23}$$

And the time dependency of the contact area is given by

$$\overline{a}(t)=[\overline{F}(t)\cdot\overline{\phi}(t)]^{1/3} \tag{24}$$

As the total pressure is given by $F_N(t)=F_N\overline{F}(t)$, where $\overline{F}(t)$ follows a Heaviside function, the solution of the viscoelastic orthotropic contact can be expressed as the product of the contact solutions in time and space [10]. The contact area is given by an elliptical contact area of axes $a_x(t)$ and $a_y(t)$ given by

$$a_x(t)=\left(\frac{3RF}{4}\right)^{1/3}[I_1\cdot\overline{\phi}(t)]^{1/3}, \tag{25}$$

$$a_y(t)=\left(\frac{3RF}{4}\right)^{1/3}\left(\frac{I_2^{1/2}}{I_1^{1/6}}\right)[\overline{\phi}(t)]^{1/3}, \tag{26}$$

The creep compliance function, $\overline{\phi}(t)$, has been normalised with respect to the fully relaxed compliance, ϕ_r. Therefore, in the elastic case, the normalised creep compliance function will be constant and unity, $\overline{\phi}(t)=1$. From the definition of creep compliance in [6], the contact area in the viscoelastic isotropic case is given by

$$a(t)=\left(\frac{3RF}{4}\right)^{1/3}\left[\frac{1-\nu^2}{E}\cdot\overline{\phi}(t)\right]^{1/3} \text{ or } a(t)=\left(\frac{3RF}{4}\right)^{1/3}\left[\frac{\overline{\phi}(t)}{2}\right]^{1/3} \tag{27}$$

4. Results and discussion

To compare the results that are obtained using the newly developed orthotropic viscoelastic isochronous contact model with both elastic anisotropic and isotropic viscoelastic models available in literature, the elastic and viscoelastic properties of EPDM will be considered as reference. The elastic material properties were measured for EPDM samples by employing a tensile tester, whilst the viscoelastic properties were characterised using Dynamic Mechanical Analysis (DMA). The mean creep compliance of the material is expressed as a series of discrete exponential terms [15] given by

$$\overline{\phi}(t)=\overline{\phi}_r-\sum_{i=1}^{3}\overline{\phi}_i\exp\left(\frac{-t}{\lambda_i}\right) \tag{28}$$

where ϕ_r indicates the creep compliance at a fully relaxed state and λ_i indicates the retardation times. For the EPDM used in this study, the elastic modulus is E=4.39 MPa and the creep parameters are summarised in Table 1.

The results discussed in following paragraphs refer to an indenter with a radius of R=12.5 mm that is pressed against a viscoelastic anisotropic EPDM body at an applied load F_N=2 N.

4.1. Influence of the normalised creep function

In Eq. (27) the elastic behaviour is represented by the Young's modulus E and the viscous behaviour by the normalised creep compliance $\overline{\phi}(t)$. To study the influence of the viscous or time dependent behaviour, the normalised creep functions of several materials (EPDM, PU [14], PMMA [16] and PC [16]) are presented in Fig. 2. These normalised creep functions will be multiplied with the elastic properties of EPDM to calculate the contact area; the results are shown in Fig. 3. Fig. 2 shows that at long times scales the creep compliance function for all materials approaches unity. The speed of this approach depends mainly on the retardation times of the creep function. The normalised creep function for a purely elastic material (i.e. $\phi(t)/\phi_r=1$) is also shown.

Table 1
Compliance coefficients and Retardation times for EPDM.

i	ϕ_i (Pa^{-1})	λ_i (ms)
ϕ_r	3.493×10^{-7}	
1	4.692×10^{-8}	6.4
2	4.903×10^{-8}	71.3
3	8.232×10^{-8}	728.4

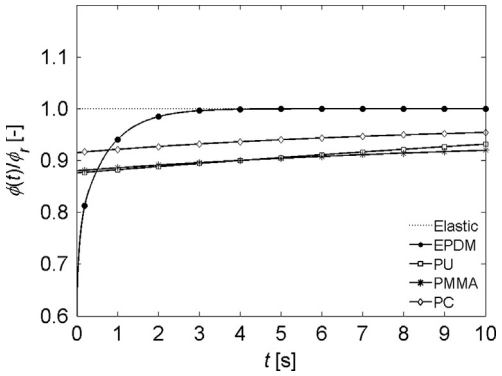

Fig. 2. Normalised creep functions for different materials.

The time dependency of the contact area is influenced by the normalised creep compliance, but the magnitude of the contact area is influenced by the elastic material parameters applied [9,10].

It can be concluded that the relevance of a viscoelastic contact model is highly dependent on the time-scale at which the contact occurs in relation with the characteristic retardation times of the viscoelastic material.

4.2. Influence of the elastic modulus in the plane of indentation (E_x)

The influence of a reinforcement of the material in the plane of indentation on the contact area is illustrated in Fig. 4. The reinforcement is applied as an increase of the elastic modulus in one direction (x) of the x–y indentation plane without changing the other elastic moduli, shear moduli or Poisson's ratios. The black solid line in Fig. 4(a) shows the contact area for the isotropic case and the solid lines with markers show the contact areas for various reinforcements of E_x. It can be seen that reinforcement results in the contact area to decrease slightly with increasing E_x. Fig. 4(b) shows the circularity or roundness of the contact area, i.e. the ratio between the two primary axes of the contact area. A circularity of 1.0 means that the contact area is circular and deviating values indicate an elliptic shape of the contact area. The contact area, which is circular for isotropic materials, becomes increasingly elliptically shaped with increasing E_x.

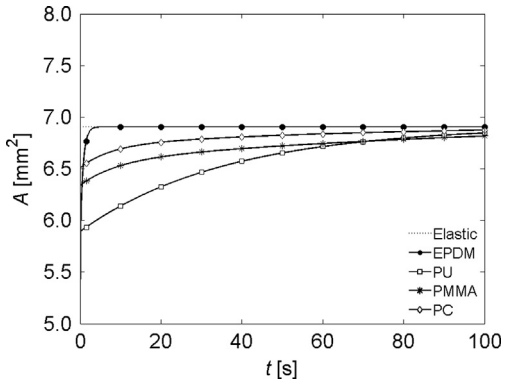

Fig. 3. Influence of normalised creep compliance on the contact area.

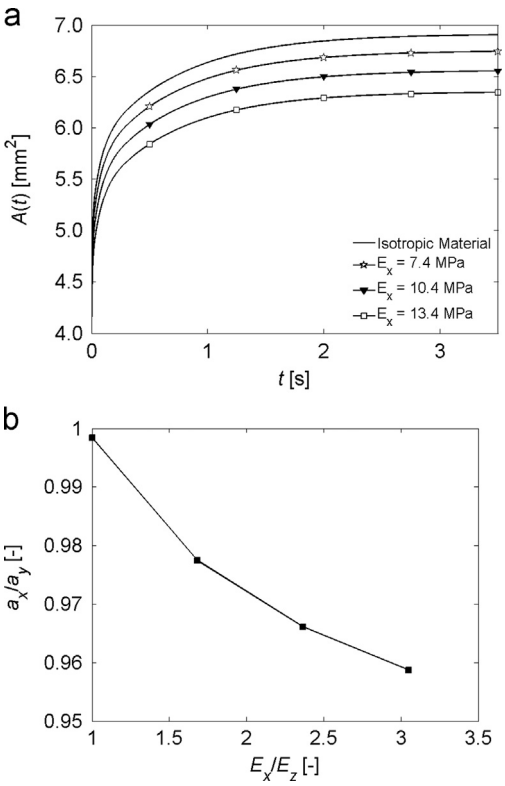

Fig. 4. (a) Influence of increasing the elastic modulus in the indentation plane on the contact area and (b) effect of different degrees of reinforcement on the circularity of the contact area.

The reinforcement, using fibres, of a polymer matrix will not only affect the Young's modulus E_x, but also the shear modulus G. The effects are illustrated in Fig. 5, in which the shear moduli in different directions are varied from being constant to be dependent on E_x, according to $G=E_x/2(1+\nu)$. Fig. 5(a) shows that an increase of the shear modulus results in a significant decrease of the contact area, the effect being strongest for an increase of G_{xz}. Fig. 5(b) shows that a change of the shear modulus also affects the elliptical shape of the contact area.

4.3. Influence of elastic modulus in the direction of indentation (E_z)

Fig. 6 shows the influence of the elastic modulus in the direction of indentation of the material on the contact area. In Fig. 6(a) the isotropic case is represented by a solid black line, and increasing E_z is represented by dashed lines. It can be seen that the contact area

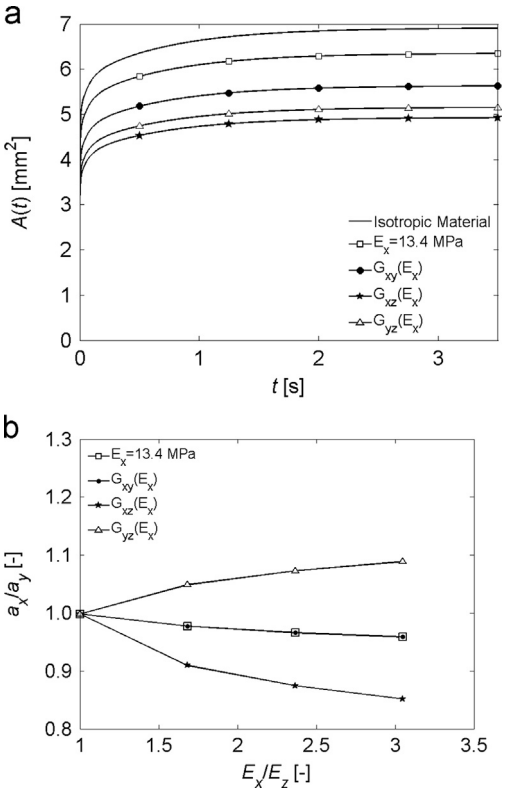

Fig. 5. (a) Influence of increasing the shear moduli on the contact area and (b) effect of different shear moduli on the circularity of the contact area.

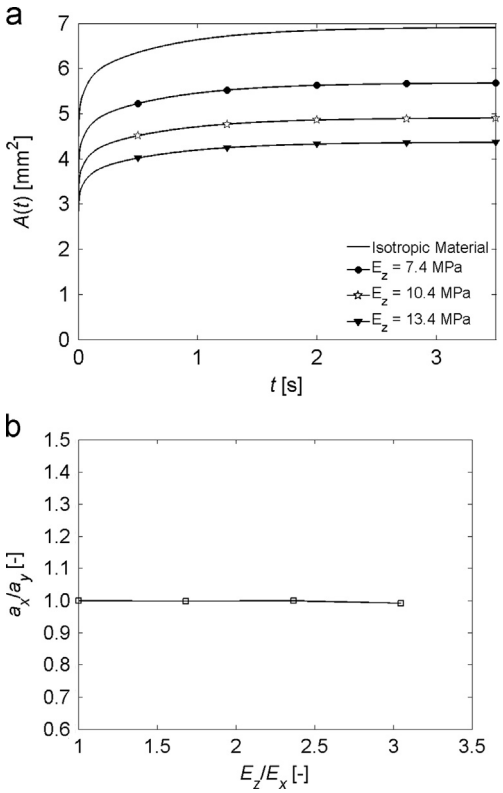

Fig. 6. (a) Influence of increasing E_z on the contact area and (b) effect of increasing E_z on the circularity of the contact area.

decreases significantly with increasing the elastic modulus in the direction of indentation (E_z). Comparing Fig. 6(a) with Fig. 4(a) shows that increasing E_z has a stronger effect than increasing E_x. Fig. 6

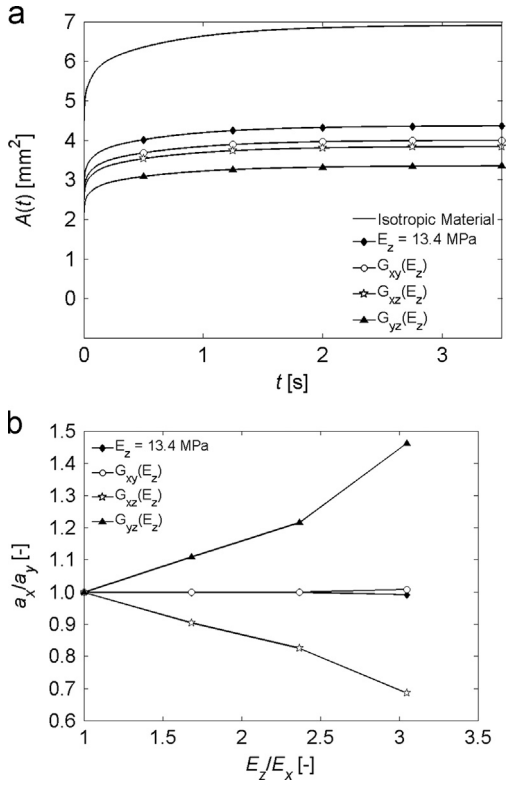

Fig. 7. (a) Influence of different shear modulus on the contact area and (b) effect of shear modulus on the circularity of the contact area.

shows that an increase of the elastic modulus in the direction of indentation, has no effect on the shape of the contact area, which remains circular.

In Fig. 7(a), it is shown that an increase of any of the shear modulus causes a decrease of the contact area. In the different dashed lines each shear modulus varies as $G=E_z/2(1+\nu)$, whilst the other shear modulus remain constant. Each shear modulus affects the contact area with different magnitudes depending on the direction of the shear modulus, as seen in Fig. 7(b). Different directions of shear modulus can affect the shape of the contact area, from circular to elliptical, as seen in Fig. 7(b).

4.4. Comparison with viscoelastic isotropic contact models

Ting [6] describes a contact model for isotropic viscoelastic materials. For the controlled load case, in which the normal load follows a Heaviside step function, Ting's radius of the contact area is defined as

$$a(t)=\left[\frac{3RF_N}{8}\phi(t)\right]^{1/3} \tag{29}$$

Fig. 8 shows the results of a comparison between the newly developed orthotropic viscoelastic isochronous contact model and the isotropic viscoelastic contact model of Ting [6], using the elastic and viscoelastic material parameters measured for EPDM. The contact area shows a small difference of 0.35% between the two models, which is only to be expected, as the models use different input parameters. The input parameters required by the orthotropic viscoelastic isochronous contact model are more numerous and are determined with a range of different tests, compared to the single input parameter of the Ting model. Therefore, it can be concluded that, when used for isotropic

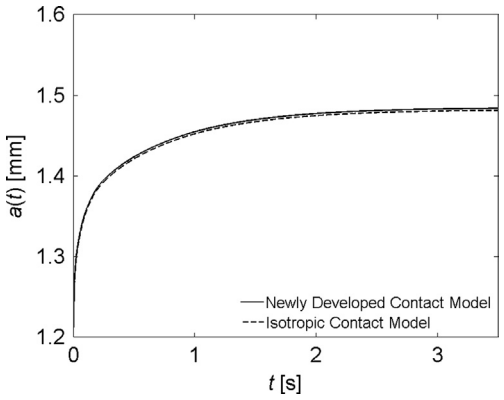

Fig. 8. Comparison of the orthotropic viscoelastic isochronous contact model with the isotropic viscoelastic contact model of Ting [6].

Table 2
Elastic properties of woven glass/epoxy composite [17].

E_x (warp) (GPa)	E_y (Fill) (GPa)	G_{xy} (GPa)	G_{xz} (GPa)	G_{yz} (GPa)	ν (–)
21.95	21.8	3.52	1.84	1.72	0.08

materials, the results of the orthotropic viscoelastic anisotropic contact model agree with the results found in literature.

4.5. Viscoelastic anisotropy

To study the viscoelastic anisotropic contact model, an analysis of a composite material made of FR-4 epoxy matrix reinforced with 7628 woven glass fabric is made. The anisotropic elastic properties of this composite have been described by Hutapea and Grenestedt [17], shown in Table 2, while Shrotriya et al. [18] characterised the viscoelastic properties, shown in Table 3.

Fig. 9 shows the calculated contact area the woven glass epoxy composite in contact with a spherical indenter with a radius of 5 mm, at a normal load of 1 kN. The contact area was calculated under three configurations

- The orthotropic case, calculated with the newly developed orthotropic viscoelastic contact model, by using the elastic material parameters listed in Table 2 and the normalised creep compliance defined by the parameters in Table 1 (shown in solid black squares).
- The isotropic case, calculated with the newly developed orthotropic viscoelastic contact model, by using the elastic material parameters corresponding to the warp direction, E=21.95 GPa and G=3.52 GPa and the normalised creep compliance (shown in white squares).
- The isotropic case by using Ting's unidirectional viscoelastic contact model, with as input parameters the (non-normalised) creep compliance function of the composite in the warp direction, defined by the parameters in Table 1 (shown in asterisks).

The difference between the orthotropic contact area and the contact area calculated using the creep compliance in the warp direction is 23%. This can be explained by the large influence of the shear moduli in each direction. Discounting these effects, i.e. by using an isotropic viscoelastic contact model, will overestimate the shear modulus of the material and thus predict a lower contact area than an orthotropic viscoelastic contact model. Indeed,

Table 3
Retardation times λ and compliance coefficients ϕ for woven glass/epoxy in the warp direction [18].

i	ϕ_i (GPa^{-1})	λ_i (min)
ϕ_r	1.26×10^{-1}	
1	3.81×10^{-3}	1.61×10^{1}
2	5.48×10^{-3}	5.55×10^{2}
3	2.29×10^{-3}	9.09×10^{3}
4	5.62×10^{-3}	6.25×10^{4}
5	1.32×10^{-2}	6.89×10^{5}
6	1.33×10^{-2}	6.06×10^{6}
7	1.55×10^{-2}	1.00×10^{8}
8	1.05×10^{-2}	5.49×10^{8}
9	1.57×10^{-2}	5.00×10^{9}

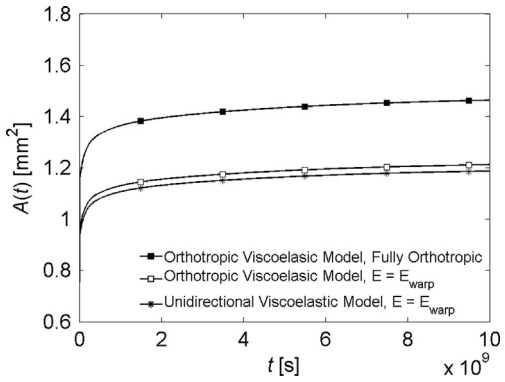

Fig. 9. Contact area calculated for the woven glass epoxy composite.

employing the orthotropic viscoelastic contact model with material properties in the warp direction, i.e. the indentation direction, results in similar low contact areas, as illustrated by the white squares Fig. 9. The difference between the calculated contact areas using the isotropic case in the warp direction and the unidirectional viscoelastic model of Ting is about 2%. When applied to an anisotropic, viscoelastic material, the use of an isotropic model will overestimate the stiffness and result in a contact area that is too small.

5. Conclusions

A model describing the contact behaviour of orthotropic viscoelastic materials was developed by separating the temporal and spatial variables. Employing this newly developed contact model enables the study of the influence of various material properties in the principal directions (x, y, z) and the influence of the viscoelastic behaviour of the material. The model employs one normalised creep compliance function for the mechanical properties, i.e. the viscoelastic behaviour is modelled isochronously.

The viscous behaviour of the material is modelled using the normalised creep function, which influences the contact area by means of the retardation times, without modifying the eventual magnitude of the contact area. The influence of an increased elastic modulus in one direction in the plane of indentation was studied, and it was found that the contact area only decreases slightly. However, because the Young's modulus also affects the shear modulus, the contact area for such a material may decrease significantly. In the direction of indentation, an increase of the elastic modulus causes a significant decrease of the contact area, whilst the shear modulus influences the shape of the contact area, which can vary from circular to elliptical depending on the direction of the shear modulus. Results obtained using the newly developed orthotropic viscoelastic isochronous contact model are in line with results described in literature, both for isotropic and anisotropic materials.

Acknowledgements

This work is part of the Research Programme of the Dutch Polymer Institute DPI, The Netherlands, Project nr. #664. The authors are grateful to C. Hintze of the Leibniz Institute for Polymer Research, Dresden, Germany for providing the tensile data of the EPDM and to M. Sadatshirazi from the University of Twente for providing the EPDM samples.

Appendix A. A fully anisotropic contact model

Willis [9] solves the effect of a point load on an anisotropic half space, and later uses the solution to solve the effect of a certain pressure distribution on an anisotropic half space.

The problem is defined by the stress equilibrium equation (where σ indicates the stresses, repeated subscript denotes summation, comma denotes differentiation), the stress–strain equation for anisotropic materials, and the boundary conditions.

$$\sigma_{ij,j} = 0 \text{ and } \sigma_{ij} = c_{ijkl} u_{k,l} \quad \text{for } z \geq 0 \tag{A.1}$$

$$\sigma_{zz} = -\delta(x)\delta(y) F_N \quad \text{for } z = 0 \tag{A.2}$$

Combining the two equations and introducing the convention that Latin suffixes take values of x, y, z and Greek suffixes take values of x, y

$$c_{i\alpha k\beta} u_{k,\alpha\beta} + (c_{i\alpha kz} + c_{izk\alpha}) u_{k,\alpha z} + c_{izkz} u_{k,zz} = 0 \tag{A.3}$$

Taking the Fourier transform in the x and y-directions, denoting $\xi = (\xi_1, \xi_2)$ as the Fourier transform parameters and $\mathrm{x} = (\mathrm{x}, \mathrm{y})$, the displacement in the Fourier domain is

$$\tilde{u}_k(\xi, z) = \sum_{A=1}^{6} a_{k^A}(\xi) \exp[i m_A(\xi) z] \tag{A.4}$$

where

$$\left[c_{izkz} m_A^2 + (c_{i\alpha kz} + c_{izk\alpha}) \xi_\alpha m_A + c_{i\alpha k\beta} \xi_\alpha \xi_\beta\right] a_{k^A} = 0 \tag{A.5}$$

m_A is one of the six roots, obtained by setting the determinant of the matrix in Eq. (A.5) to zero. As the displacement must be finite far from the load, only the roots with positive imaginary parts are retained. By substituting these roots back in Eq. (A.5) the first two rows of the ratios a_{1^A}/a_{3^A} and a_{2^A}/a_{3^A} are obtained. By applying the Fourier transform to the boundary conditions and substituting Eq. (A.4), the remaining constants are obtained

$$\sum_{A=1}^{3} [m_A (a_{1^A}/a_{3^A}) + \xi_1] a_{3^A} = 0 \tag{A.6}$$

$$\sum_{A=1}^{3} [m_A (a_{2^A}/a_{3^A}) + \xi_2] a_{3^A} = 0 \tag{A.7}$$

$$\sum_{A=1}^{3} [c_{xxzz} \xi_1 (a_{1^A}/a_{3^A}) + c_{yyzz} \xi_2 (a_{2^A}/a_{3^A}) - c_{zzzz} m_A] a_{3^A} = \frac{-i}{\pi} \tag{A.8}$$

And the normal displacement in $z = 0$ due to a concentrated normal load is known in its Fourier transform as

$$\tilde{u}_z(\xi, 0) = \sum_{A=1}^{3} a_{k^A}(\xi) \tag{A.9}$$

By inverting this Fourier transform, assuming that the contact area is an ellipse with principal axes (a_x and a_y) and with a

pressure distribution given by

$$p(x,y) = p_0\left(1-\frac{x^2}{a_x^2}-\frac{y^2}{a_y^2}\right)^{1/2} \tag{A.10}$$

The normal displacement can be solved by numerically, by evaluating the following contour integral

$$u_z(x,y,0) = p_0\frac{\pi a_y}{4}\int_0^{2\pi}\tilde{u}_z\left(\frac{a_y}{a_x}\cos\theta,\ \sin\theta\right)\cdot\left[1-\left(\frac{\cos\theta\, x}{a_x}+\frac{\sin\theta\, y}{a_y}\right)^2\right]d\theta \tag{A.11}$$

The contact area can be expressed by

$$a_x = \left(\frac{3RF_N}{4}\right)^{1/3} I_1^{1/3} \text{ and } a_y = \left(\frac{3RF_N}{4}\right)^{1/3}\frac{I_2^{1/2}}{I_1^{1/6}} \tag{A.12}$$

where

$$I_1 = \int_0^{2\pi}\tilde{u}_z(\varepsilon\cos\theta,\ \sin\theta)\cdot(\cos\theta)^2 d\theta \tag{A.13}$$

$$I_2 = \int_0^{2\pi}\tilde{u}_z(\varepsilon\cos\theta,\ \sin\theta)\cdot(\sin\theta)^2 d\theta \tag{A.14}$$

More details of this procedure can be found in Willis [9] and Swanson [10].

References

[1] Johnson KL. Contact mechanics. Cambridge: Cambridge University Press; 1985.
[2] Hertz H. Über die Berührung fester elastischer Körper. J. reine u. angewandte Math 1881;92:156–71.
[3] Lee EH, Radok JRM. The contact problem for viscoelastic bodies. J. Appl. Mech. 1960;27:438–44.
[4] Graham GAC. The contact problem in the linear theory of viscoelasticity. Int. J. Eng. Sci. 1965;3:27–46.
[5] Graham GAC. The contact problem in the linear theory of viscoelasticity when the time dependent contact area has any number of maxima and minima. Int. J. Eng. Sci. 1967;5:495–514.
[6] Ting TCT. The contact stress between a rigid indenter and a viscoelastic half-space. J. Appl. Mech. 1966;33:845–54.
[7] Green AE, Zerna W. Theoretical elasticity. Oxford: Oxford University Press; 1954.
[8] Dahan M, Zarka J. Elastic contact between a sphere and a semi infinite transversely isotropic body. Int. J. Solids. Struct. 1977;13:229–38.
[9] Willis JR. Hertzian contact of anisotropic bodies. J. Mech. Phys. Solids. 1966;14:163–76.
[10] Swanson SR. Hertzian contact of orthotropic materials. Int. J. Solids Struct. 2004;41:1945–59.
[11] Yang SH, Sun CT. Indentation law for composite laminates. In: Daniel IM, editor. Composite materials: testing and design, 6th conference. ASTM STP 787; 1982. p. 425–449.
[12] Tan TM, Sun CT. Use of statical indentation laws in the impact analysis of laminated composite plates. J. Appl. Mech. 1985;5:6–12.
[13] Rodriguez NV, Masen MA, Schipper DJ. A model for the contact behaviour of weakly orthotropic viscoelastic materials. Int. J. Mech. Sci., http://dx.doi.org/10.1016/j.ijmecsci.2013.03.016, in press.
[14] Deladi EL. Static friction in rubber–metal contacts with application to rubber pad forming processes. PhD thesis, University of Twente, Enschede, The Netherlands, 2006.
[15] Ferry JD. Viscoelastic properties of polymers. New York.John Wiley and Sons; 1980.
[16] Lu H, Wang B, Ma J, Huang G, Viswanathan H. Measurements of creep compliance of solid polymers by nanoindentation. Mech. Time-Depend. Mat. 2003;7:189–207.
[17] Hutapea P, Grenestedt J. Effect of temperature on elastic properties of woven-glass epoxy composites for printed circuit board applications. J. Electron. Mater. 2003;32(4):221–7.
[18] Shrotriya P, Sottos NR. Creep and relaxation behavior of woven glass/epoxy substrates for multilayer circuit board applications. Polym. Compos. 1998;19(5):567–78.